17th World Conference on Earthquake Engineering, 17WCEE
Sendai, Japan - September 13th to 18th 2020

CYCLIC TESTS OF CONCRETE–LOW-YIELD STEEL COMPOSITE WALLS SUBJECTED TO IN-PLANE SHEAR AND AXIAL LOADS

Chin-Tung Cheng [(1)], Yung-Chin Chang [(2)], and Heui-Yung Chang[(3)]

[(1)] *Professor, Department of Constriction Engineering, National Kaohsiung University of Science and Technology, Taiwan, ctcheng@nkust.edu.tw*
[(2)] *Graduate Student, Department of Civil and Environmental Engineering, National Kaohsiung University, Taiwan, jackchang274@gmail.com*
[(3)] *Professor, Department of Civil and Environmental Engineering, National Kaohsiung University, Taiwan, hychang@nku.edu.tw*

Abstract

The concrete-steel composite walls are made of two low-yield steel faceplates sandwiched concrete infill with shear studs in inner wall anchoring steel faceplates through concrete infill. In addition, shear studs have the function of postponing the buckling of steel faceplates and extending the tension field of the steel faceplates. Since the composite walls have very good stiffness and strength, it was extensively used in nuclear power plants to resist lateral forces and ice-resisting wall for arctic offshore structures and ship hulls. This research aims to investigate seismic performance of the composite walls subjected to cyclic in-plane shear and axial loads for its application in high-rise buildings.

In this research, eight specimens were constructed and tested, having the same aspect ratio of 1.0 with size of 1200x1200 mm. The application of low-yield steel for composite shear walls is rarely seen from literature, as well as the walls subjected to high axial loads. The advantage of low-yield steel is the enlargement of both energy dissipation for the walls as well as the spacing of shear studs used in the inner walls. In addition, the axial load effect on the seismic behavior of walls should be clarified before its application in high-rise buildings. Compared with static loading protocol, a near-fault loading protocol was applied to investigate the effect of loading rate. In summary, the investigating parameters in this research include thickness of the concrete infill, spacing of shear studs, level of axial load, and lateral loading rates such as static or near-fault dynamic loading.

Test results show that axial load may have marginal effect on the ultimate strength of composite walls. However, it may significantly affect its post-peak ductility. Under high level of axial loads, the failure modes for specimens with shear studs spacing suggested by literature, which did not account for axial loads, resulted from diagonal buckling of steel faceplate due to insufficient anchor of shear studs inside walls, that significantly reduced its post-peak ductility of the walls. For specimen with less shear studs spacing, the failure modes focused on local buckling of steel faceplate between shear studs, especially at top and bottom ends of the specimens. In this case, the ductility of the walls may be extensively increased, having largest energy dissipating capacity. Under low level of axial loads, the failure modes transformed from shear to flexure that largely increased the ductility of the walls. Test results also reveal that the thickness of the composite walls has marginal effect on seismic performance of the walls. However, the specimen with 15 cm thick concrete infill have better performance than those with 10 cm thick concrete in terms of buckling of steel faceplate. It is found that the near-fault loading may increase approximately 5% of lateral strength with similar ductility for the composite walls.

Keywords: Composite shear wall, shear studs, low-yield steel, concrete infill, axial load, and cyclic behavior.

1. Introduction

Concrete-filled double-skin composite walls (CDCWs) have been used in the ice-resisting wall for Arctic offshore structures (Ohno et. al. 1987[1], Matsuishi and Iwata, 1987[2]), ship hulls (Huang et al. 2014[3]), nuclear power plants (Fukumoto et al. 1987[4], Ozaki et al. 2004[5], Rahai and Hatami, 2009[6], Vecchio and McQuade, 2011[7], Danay, 2012[8], Varma, 2014[9], Epackachi et al. 2015[10-11], Seo et al. 2016[12], Kurt et al. 2016[13], and Yan and Liew, 2016[14]), and shear walls in buildings (Eom et al. 2009[15], Hu et al., 2014[16], Nie et al. 2013[17], Nie et al. 2014[18], Chen et al. 2015[19], Ji et al. 2017 [20] and Zhao et al. 2016[21]). Experimental investigation in literature showed that CDCWs exhibited excellent lateral strength and deformation capacity. CDCWs consist of structural steel modules that are filled with plain or high strength concrete to develop composite systems. As shown in Fig. 1 (Epackachi et al. 2015a[10]), the steel modules are composed of (i) two steel faceplates that form the surfaces of the CDCWs, (ii) uniformly distributed shear studs on the inside surfaces of the steel faceplates, and (iii) tie bars or rods connecting the two faceplates together (Seo et al. 2016[12]) . The shear studs provide composite action for steel faceplates and concrete infill, and the tie bars fasten two steel faceplates serving as formwork for the pouring of concrete infill. The steel modules can be fabricated in shops with quality control, and shipped to the site for assembly. CDCWs can improve the construction efficiency and economy over conventional reinforced concrete (RC) construction.

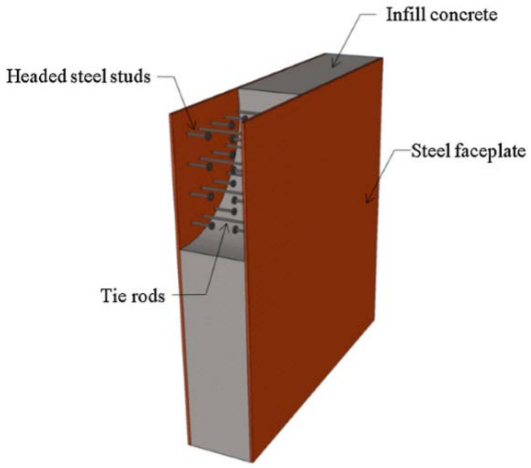

Fig. 1 Typical cross section of concrete filled steel plate shear walls (Epackachi et al. 2015a[10])

Experimental studies have been conducted in Japan, S. Korea, Mainland China, and the US to investigate the in-plane shear behavior of CDCWs. These researches have focused on the pure in-plane shear behavior of CDCW panels which may be used in commercial building construction and safety-related nuclear facilities. To avoid the welding failure of steel faceplates at the base, specimens in literature were embedded in a concrete foundation and loaded at the top of specimens in a cantilever way, resulting in large moment demand at the specimen base. Therefore, the behavior of CDCWs without the support of boundary elements is governed by the flexure failure at the base due to the crushing of concrete and buckling of steel faceplates, and shear failure does not occur for wall aspect ratios greater than or equal to 0.60 (Seo et al. 2016). In this paper, wall specimens are surrounded by boundary elements and tested by a new setup that deforms the specimen in double curvature. The specimens may be failed by shear in yielding of steel faceplate rather than literature's flexural buckling, benefited from the decrease of the flexural moment at top and bottom wall boundary.

Low-yield steel has the advantage of extending the ductility of steel faceplate and reducing the amount of shear studs used in inner walls. However, it is not gained attention in the application of low-yield steel on composite walls till now. Besides, it is important to clarify the axial load effect on the seismic behavior of

walls before its application in high rise-buildings. In the research of Ji et. al. 2017[20], experimental and analytical investigation indicated that axial compression has limited influence on the shear strength, but decreases the shear-deformation capacity of the composite walls. The high axial load may potentially lead to the crushing of concrete infill prior to the yielding of the steel faceplate.

Therefore, the objective of this research is to investigate in-plane shear performance of concrete-filled low-yield-steel-plate composite walls in high-rise buildings. To validate the proposed idea, six reduced-scale composited walls were constructed and tested by a new established test setup at Tainan Lab. National Center for Earthquake Engineering (NCREE) in Taiwan. Seismic response of structures varied with investigating parameters is evaluated.

2. EXPERIMENTAL PROGRAMS

As shown in Fig. 2, all specimens have aspect ratio of 1.0, in which two specimens have the dimension of 1200X1200X106 mm in size that is reduced approximately 2.5 times from a prototype structure with story height 3000 mm and wall thickness of 250 mm, respectively. Table 1 shows the specimen design and investigated parameters. The reinforcement ratio of composite walls in safety-related nuclear facilities is ranging 1.5-5% with head to head shear studs in inner shear walls as shown in Fig. 1. In this paper, two 8 mm thick low-yield steel faceplates sandwiched 10 cm or 15cm thick concrete infill and connected by interlaced shear studs, having 13.8% or 9.6% reinforcement ratio, respectively as shown in Figs. 3-5. Since the shear studs were interlaced, the reinforcement ratio in this paper should be divided by two, when compared with head to head shear studs as shown in Fig.1. The slenderness ratio of steel faceplate is 30 for specimens with 24 cm spacing of shear studs in inner walls. This ratio is far less than required slenderness ratio of 44.7, which is calculated on the basis of the research by Zhang et al. 2014 [22] as

$$\frac{S}{T_p} = \sqrt{\frac{E_s}{F_y}} \tag{1}$$

where S is the spacing of shear studs or bolts, and E_s and F_y elastic modulus and yield strength for steel faceplates, respectively. To account for the strain hardening effect of steel faceplate, the required slenderness ratio of 31.6 is calculated by replacing yield strength Fy of steel faceplate with tensile strength Fu=200MPa in equation (1). The tensile strength Fu is obtained from stress-strain curve of low-yield steel by a target drift ratio 4% that the wall may experience under extreme loads. In Table 1, the required slenderness ratio of 25.3 for specimens with 20cm spacing of shear studs is calculated in a more congregative way by multiplying 0.8 to 31.6.

In literature, test specimens were embedded in a concrete foundation to avoid the welding failure of steel faceplates at the base. Without the support of boundary elements, the behavior of CDCWs is governed by the flexure failure at the base due to the crushing of concrete and buckling of steel faceplates. In this paper, wall specimens were installed to the test machine through the top and base steel plates. To mitigate the concrete crushing during tests, a 10 mm steel plate acted as boundary element for composite walls was applied to protect the concrete infill from crushing. In all interfaces, full penetration welds were applied to connect walls to the base plates and wall boundary. To avoid the welding failure at the interface, stiffener plates were used as shown in Fig. 2. Figures 3 and 4 show the different views of shear studs arrangement for specimens with studs spacing of 24 cm; while Figure 5 for specimens with shear studs spacing of 20 cm. Table 2 shows the material strength for the steel. The concrete was poured from a pump hole at the bottom of wall panel or the holes at the top base plate. The concrete strength at the test day was 20.4 MPa for the first four specimens; while it was 37.4 MPa for the last two specimens as shown in Table 1.

As shown in Fig. 6, all specimens were tested by Biaxial Dynamic Test System (BATS) with successive in-plane shear and constant axial loads. The specimen was fixed at the top base through high strength bolts and then applied with a constant axial load by 30000 kN vertical actuators. Then, 4000 kN actuators at the bottom base applied cyclic reversed horizontal loads with displacement control in the form of

triangular waves with strain rate of 0.003 rad/sec for the first six specimens as shown in Table 1. For specimens LBA-TC and LBA-ND, dynamic lateral loads with strain rate of 0.3 rad/sec was applied with displacement control, in which a near-fault CHICHI earthquake record TCU-084 was applied for specimen LBA-TC; while it was a synthesis near-fault earthquake recommended by the research of Lanning et al. 2016 [23] for specimen LBA-ND as shown in Fig. 7. Four transducers measured the displacement of specimens and monitored the slip in interfaces between the specimen and test facility. Before each test, strain rosettes and strain gauges were applied to monitor the strain development on the shear panel and boundary elements.

Table 1 Investigated parameters of design specimens

Specimen	Axial load ratio (P/Pu)	Thickness of whole wall T (cm)	Thickness of faceplate T_P (cm)	Reinforcement ratio T_P/T (%)	Spacing of shear studs S (cm)	Design slenderness ratio (S/T_P)	Required slenderness ratio (S/T_P)
L-B-Z-24	0	16.6	0.8	9.6	24	30	31.6
L-N-Z-24	0	11.6		13.8			
L-B-A-24	0.3	16.6		9.6			
L-N-A-24	0.3	11.6		13.8			
L-B-L-20	0.1	16.6		9.6	20	25	25.3
L-B-A-20	0.3	16.6		9.6			
L-B-A-TC	0.3	16.6		9.6			
L-B-A-ND	0.3	16.6		9.6			

Table 2 Material strength for the steel

Coupon test	Yield strength Fy (MPa)	Tensile strength Fu (MPa)
8 mm faceplate	108	272
10 mm boundary plate	273	426
25 mm top and bottom end plate	268	433

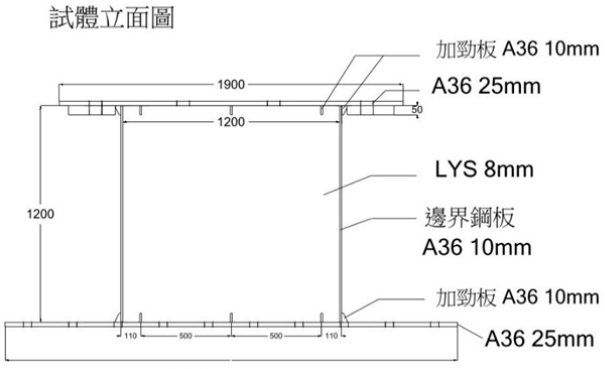

Fig. 2 Graph shows the appearance of composite walls

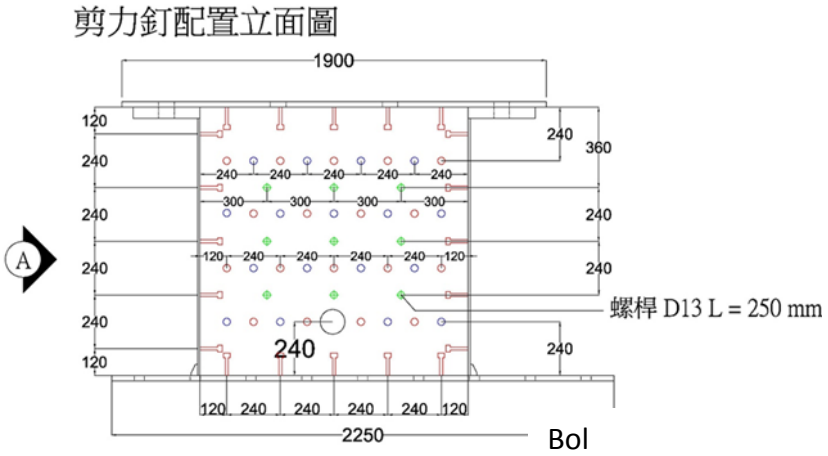

Fig. 3 Graph shows the pattern of shear studs in inner wall for specimens with studs spacing of 24 cm

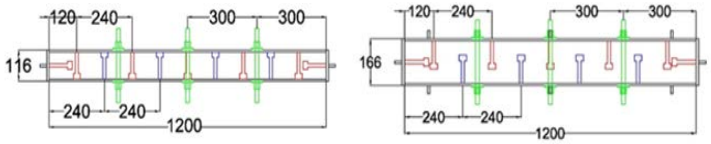

Fig 4 Graph shows the cross section of the walls for specimens with studs spacing of 24 cm

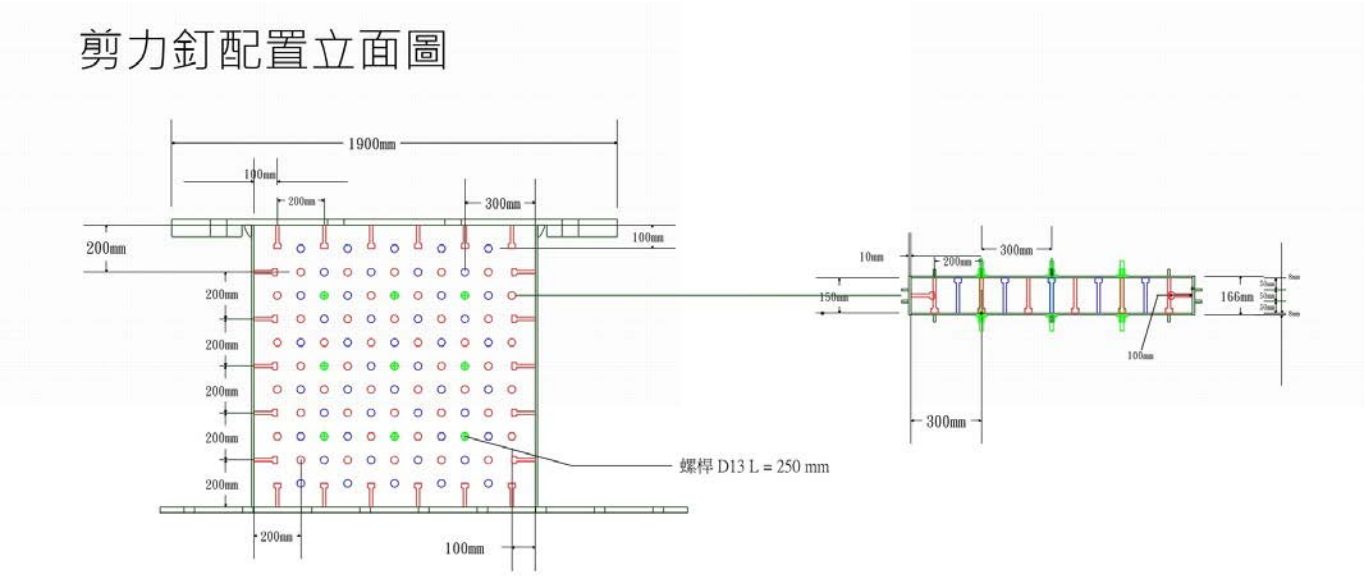

Fig 5 Graph shows the pattern of shear studs in inner wall for specimens with studs spacing of 20 cm

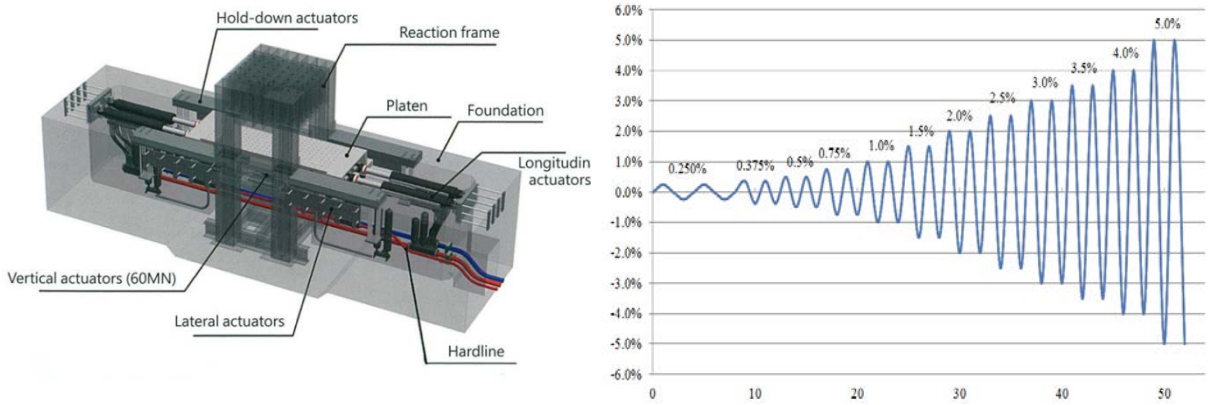

Fig. 6 Graphs respectively show the test facility (BATS) and static loading protocol

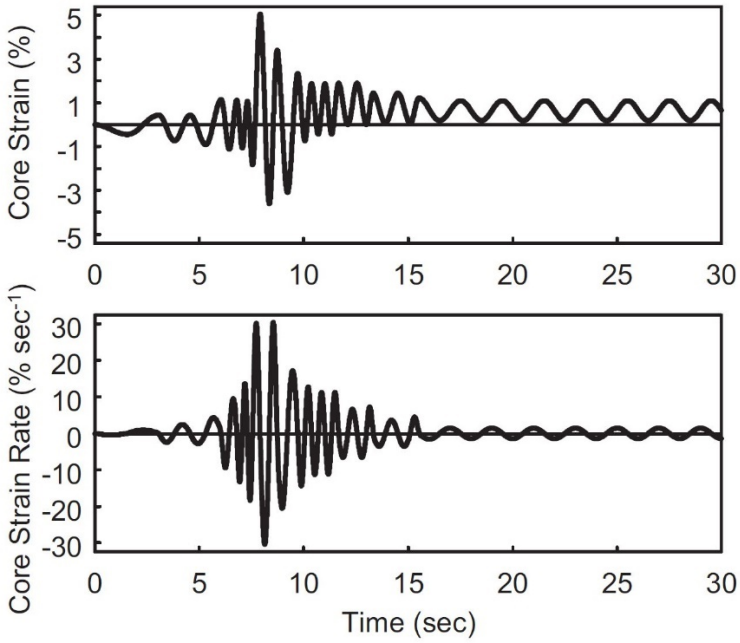

Fig. 7 Synthesis earthquake loads suggested by Lanning et al. [23]

3. TEST RESUTLS

In the test of LNZ24, plaster paint on faceplate peeled off, welding crack of left boundary plate developed near the tip of top stiffener plate, and diagonal global buckling of steel faceplate respectively occurred at the drift cycle of 0.75%, 2.5% and 3%. The lateral strength deteriorated due to the bucking of steel faceplate and test terminated at 3%. In the test of LBZ24, plaster paint on stiffener plate peeled off and welding crack of left boundary plate developed near the tip of top stiffener plate observed at the drift cycle of 0.5%, and then welding cracks on left boundary plate penetrating into the interface of top base plate and steel faceplate up to the first stiffener (110 mm from left boundary plate) at the drift cycle of 2.5%. The test terminated at the drift cycle of 3.5% due to the limit of allowable tensile displacement of axial actuators. Although the lateral strength declined, it was still larger than 85% of peak strength at the end of tests. The lateral strength deteriorated due to the welding fracture at top interface of wall and base plate.

In the tests of LNA24 and LBA24, plaster paint on stiffener plate peeled off, welding crack of left boundary plate developed near the tip of top stiffener plate, welding crack of boundary plate developed near bottom stiffener plate, and diagonal global buckling of steel faceplate respectively occurred at the drift cycle

of 0.25%, 1.0%, 1.5% and 2.0%. The lateral strength deteriorated due to diagonal global buckling of steel faceplate and test terminated at the drift cycle of 2.5%. In the tests of LBL20 and LBA20, similar failure sequence was found with cracking of boundary plate near the tip of stiffener plate penetrating into the top or bottom wall interface that lead to the crushing of the left and right corners of the wall. Local buckling of steel faceplate is more evident for the specimen with higher axial load (LBA20) than the specimen with lower axial load (LBL20). Therefore, it is found that the failure mode of specimen LBL20 is more like flexure rather than shear. For the dynamic tests of LBA-TC and LBA-ND, similar failure with specimen LBA20 was found. Although the lateral strength slightly declined, it was still larger than 85% of peak strength at the end of two tests. Fig. 8 shows the hysteretic curves for six static tests; while Fig. 9 shows the hysteretic curves for the two dynamic tests. LBA-TC was tested in gradually increase of gravity acceleration form 0.05g; while LBA-ND was amplified times from Fig. 7. Its detailed test results are summarized in Table 3, in which initial stiffness was calculated by shear strength corresponding to the drift of 0.1%, and the ultimate displacement was defined as the displacement when its lateral strength descending 85% from the peak strength.

As shown in the Table 3, with the same shear studs spacing of 24 cm, it is found that ultimate displacement of the specimens LBA24 and LNA24 with higher axial load is significantly reduced, when compared with specimens LNZ24 and LBZ24; while similar lateral strength for all specimens is obtained. For the specimens with studs spacing of 20 cm, deformation capacity of specimen LBA20 is only slightly reduced due to higher axial load, when compared with specimen LBL20; while its shear strength is increased a little. Ji et. al. 2017 [20] pointed out that composite walls made of normal strength concrete, high reinforcement ratio over 7.5% and high axial force ratios exceeding 0.4 can potentially lead to crushing of the concrete infill prior to the yielding of faceplates. This phenomena may be validated in future test, since the axial load ratio only reached 0.3 in this paper.

LNZ24

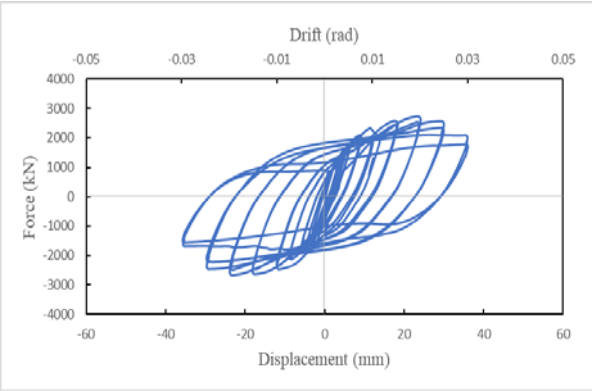

LBZ24

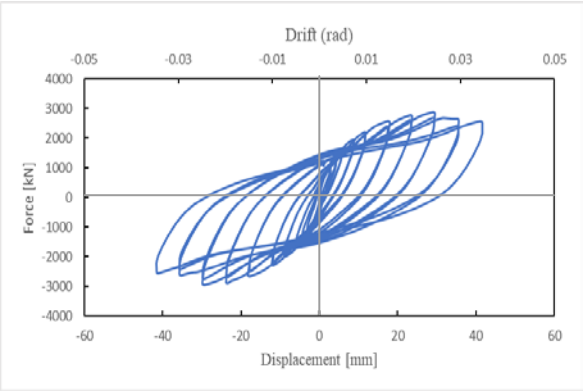

LNA24

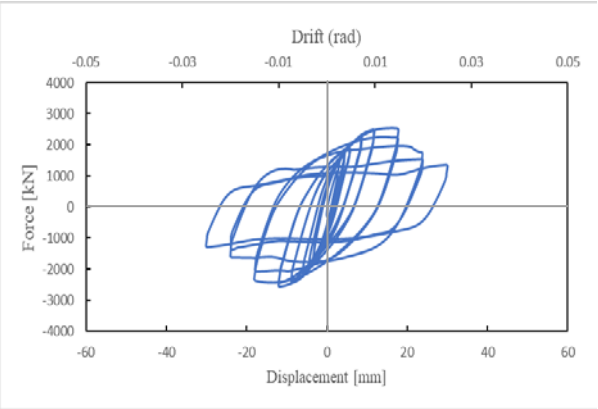

LBA24

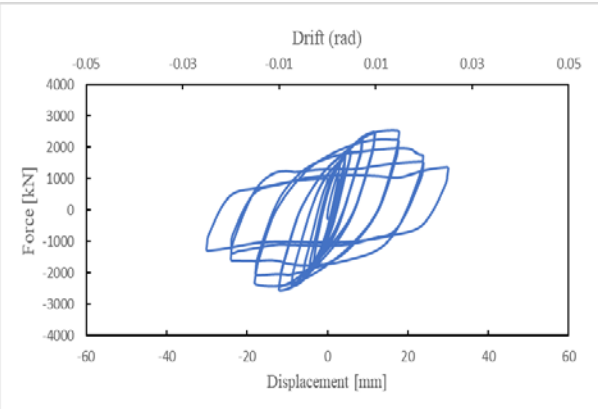

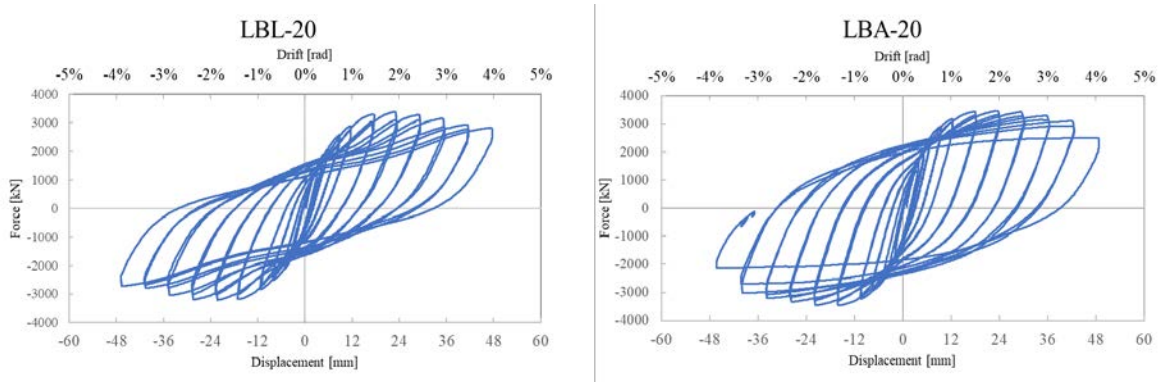

Fig. 8 Hysteretic curves for six static tests

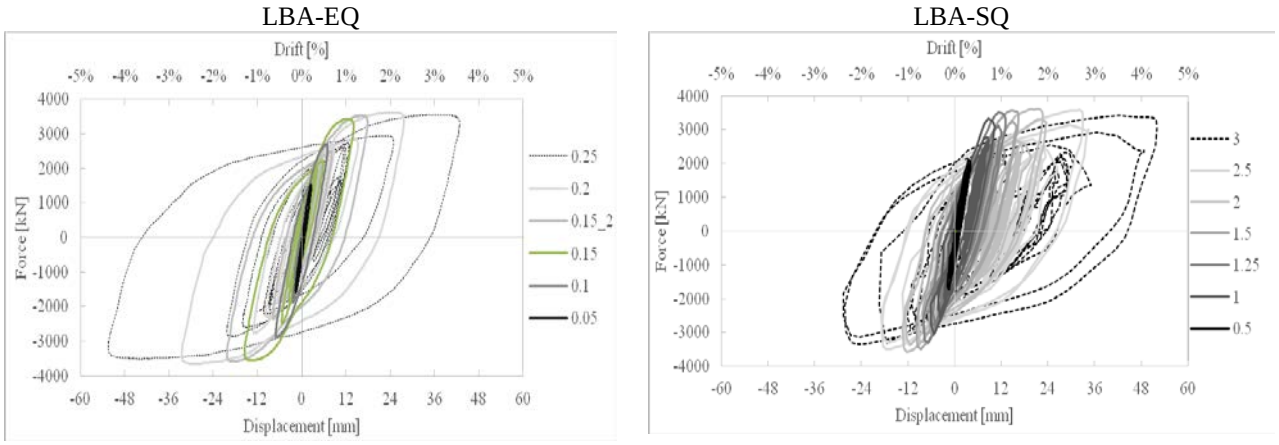

Fig. 9 Hysteretic curves for two dynamic tests

Comparison of performance between specimens LBA24 and LBA20, it is found that smaller studs spacing in specimen LBA20 has better performance in terms of both shear strength and deformation capacity. The failure mode for specimen LBA24, which has larger spacing and short length in shear studs and less concrete strength, can be characterized as diagonal global buckling of steel faceplates due to insufficient anchorage strength of shear studs. Therefore, the spacing of shear studs calculated by Equation (1) is less conservative as lateral strength reached peak strength, steel strength of faceplate may be higher than the yield strength due to strain hardening before the occurrence of buckling in faceplates. For the specimen LBA20, the spacing of shear studs is calculated in a conservative way, resulting in a better performance. It is evident that slenderness ratio has significantly influence on the seismic performance of the composite walls. Comparison of performance between specimens LBA20 and two dynamic tests, it is fount that lateral strength of dynamic tests was increased 5% with larger deformation capacity, as shown in Fig. 10.

It is found that the thickness of concrete infill (reinforcement ratio) may have marginal effect on the lateral strength and deformation capacity. The specimen LBZ24 with 15cm thick concrete infill failed due to welding fracture in the top wall interface, while specimen LNZ24 with 10 cm concrete infill failed due to diagonal global buckling of steel faceplate. It manifests that the specimen LBZ24 with 15 cm thick concrete infill may have better anchorage for the shear studs due to interlock of two heads on studs, since both specimens have the same length (10 cm) and spacing (24 cm) of shear studs. Comparison of the performance of two specimens LNA24 and LBA24 shows that lateral strength of specimen LBA24 with 15 cm thick concrete infill is 460 kN higher than that of specimen LNA24 with 10 cm thick concrete infill, while similar ultimate displacement was observed for the two specimens.

Fig. 11 shows the comparison of energy dissipation for all tests . It is found that LBA24 has largest energy dissipation capacity among static tests. For the two dynamic tests, specimen LBA-ND has larger

energy dissipation capacity than the test of LBA-TC, since it has two large pulse displacement cycles compared with only one in the test of LBA-TC.

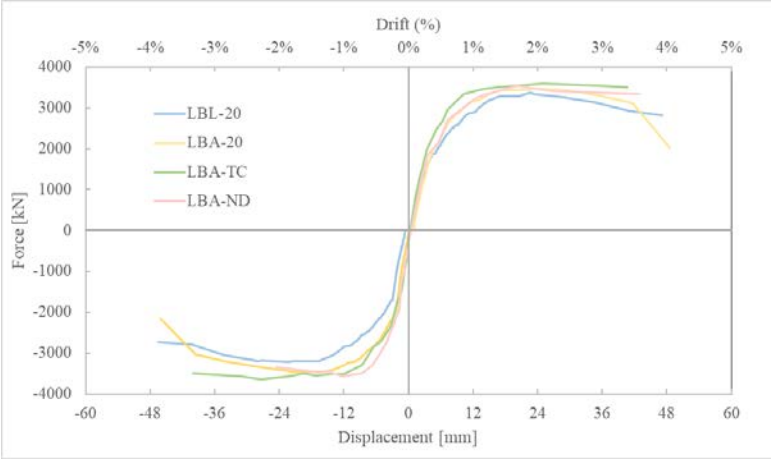

Fig. 10 Load envelop for the four specimens

Table 3 Summary of test results

Specimens	Initial Stiffness (kN/mm)	Yielding Strength		Peak Strength		Ultimate Displacement	Ductility
		Force (kN)	Δ_y (%)	Force (kN)	Δ_{max} (%)	Δ_u (%)	Δ_u / Δ_y
LNZ-24	542	+1253/ -1369	+0.27/ -0.20	+2744/ -2674	+1.96/ -1.94	+2.47/-2.47	9.2/12.2
LBZ-24	453	+1474/ -1376	+0.36/ -0.28	+2891/ -2948	+2.42/ -2.46	>+3.45/<3.45	>9.7/12.3
LNA-24	503	+1167/ -1362	+0.24/ -0.11	+2555/ -2558	+1.35/ -0.99	+1.65/-1.67	7.0/15.3
LBA-24	627	+1048/ -1527	+0.25/ -0.12	+3029/ -3014	+1.29/ -0.96	+1.60/-1.64	6.4/13.3
LBL-20	620	+1252/ -1402	+0.21/ -0.14	+3369/ -3218	+1.89/ -1.86	+3.71/-3.84	17.7/27.4
LBA-20	660	+1367/ -1603	+0.27/ -0.08	+3478/ -3467	+1.94/ -1.31	+3.56/-3.34	13.2/41.8
LBA-TC	824	+1507/ -1769	+0.21/ -0.17	+3616/ -3658	+2.04/ -2.41	>(+3.39)/ <(-3.99)	<(16.1)/ >(23.5)
LBA-ND	603	+1674/ -1643	+0.27/ -0.14	+3611/ -3577	+1.65/ -1.03	>(+3.57)/ <(-2.04)	<(13.2)/ >(14.6)

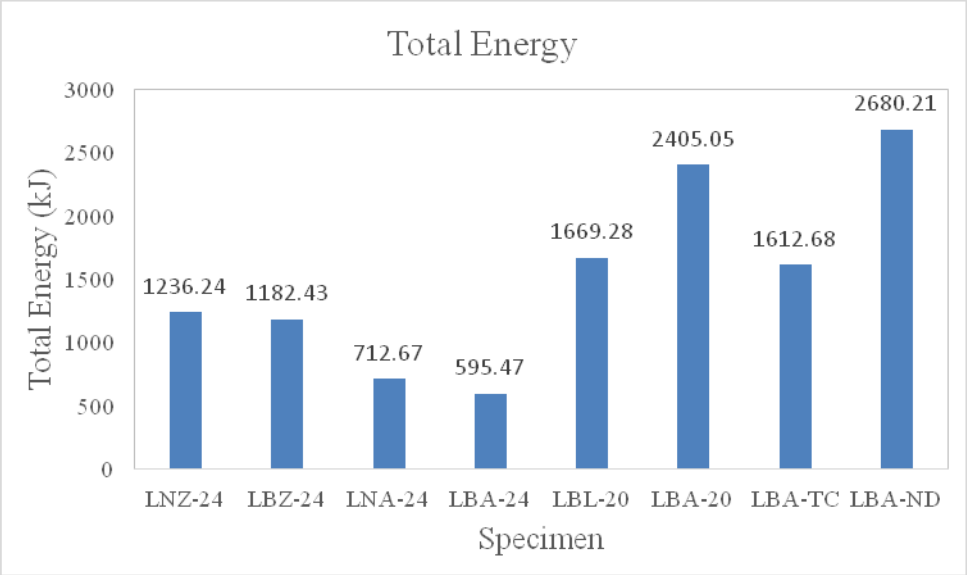

Fig. 11 Comparison of energy dissipation for all tests

4. Conclusions

Based on test results, following conclusions can be drawn:

1. With the support of boundary elements and tested by a new loading setup that deformed the walls in double curvature, the failure mechanism of specimens transformed from flexural failure that lead to the crushing of concrete infill at the base of walls as shown in literature into shear dominate with yielding or buckling of steel faceplates.
2. For the specimens with stud spacing of 24 cm, test results reveal that higher axial load significantly decreases deformation capacity of the composite walls; while it has limited influence on its lateral strength. The failure mode can be characterized as diagonal global buckling of steel faceplate due to insufficient anchorage strength of shear studs. For the specimens with studs spacing of 20 cm, it is found that higher axial load only slightly reduces deformation capacity of composite walls; while it has marginal effect on shear strength. The failure mode is characterized as flexure shear with welding crack of boundary plate near the tip of stiffener plate penetrating into the interface of steel faceplate and base plates that lead to the crushing of the left and right corners of the walls. Local buckling of steel faceplate is more evident for the specimen with higher axial load.
3. Regardless of how much axial load applied, the specimens with less studs spacing have better performance in terms of both strength and deformation capacity. It is evident that **slenderness ratio** has significantly influence on the seismic performance of the composite walls. It is found that the calculation of shear studs spacing suggested by literature is less conservative for the specimens subjected to high axial loads. Therefore, less spacing of shear studs recommended by this paper has better performance and should be used when specimens subjected high axial loads.
4. Test results show that the thickness of concrete infill (**reinforcement ratio**) may have marginal effect on the performance of composite walls, no matter what the axial load is applied. However, for the tests with zero axial loads, it is found that composite wall with 15 cm thick concrete infill did not have diagonal global buckling of steel faceplates, compared with specimen having 10 cm thick concrete infill due to insufficient anchorage of shear studs in inner wall that lead to the buckling of faceplates.
5. Test results reveal that high strain rate test in near fault loads may increase approximately 5% of lateral strength with similar ductility for the composite walls.

5. Acknowledgements

Donation of low-yield steels from China Steel Corporation is acknowledged. Financial support from National Science Council in Taiwan through grants No. MOST 107-2625-M-992-001 is greatly appreciated. The authors would also like to thank Tainan Lab, National Center for Earthquake Engineering (NCREE) in Taiwan for the assistance in experiments.

6. References

References must be cited in the text in square brackets [1, 2], numbered according to the order in which they appear in the text, and listed at the end of the manuscript in a section called References, in the following format:

[1] Ohno, F., T. Shioya, Y. Nagasawa, G. Matsumoto, T. Okada, and T. Ota (1987) "Experimental Studies on Composite Members for Arctic Offshore Structures Steel/Concrete Composite Structural Systems," C-FER Publication No. 1, Proceedings of a special symposium held in conjunction with POAC 1987, Fairbanks, Alaska, *9th International Conference on Port and Ocean Engineering under Arctic Conditions*.

[2] Matsuishi, M. and S. Iwata (1987) "Strength of Composite System Ice-Resisting Structures Steel/Concrete Composite Structural Systems," C-FER Publication No. 1, Proceedings of a special symposium held in conjunction with POAC 1987, Fairbanks, Alaska, *9th International Conference on Port and Ocean Engineering under Arctic Conditions*.

[3] Huang, Z., J.Y. Liew, Y.J. Richard, and J. Wang (2014) "Static behavior of curved lightweight steel-concrete –steel sandwich beams subjected to lateral loads." *EUROSTEEL 2014*, Naples, Italy.

[4] Fukumoto, T., B. Kato and K. Sato (1987) "Concrete filled steel bearing wall," *IABSE Symposium, Paris-Versailles*, 1987.

[5] Ozaki, M., S. Akita, H. Osuga, T. Nakayama, and N. Adachi (2004) "Study on steel plate reinforced concrete panels subjected to cyclic in-plane shear," *Nuclear Engineering and Design*, **228**, 225–244.

[6] Rahai, A. and F. Hatami (2009) "Evaluation of composite shear wall behavior under cyclic loadings," *Journal of Constructional Steel Research*, **65**, 528-1537.

[7] Vecchio, F. J., and I. McQuade (2011) "Towards improved modeling of steel-concrete composite wall elements," *Nuclear Engineering and Design*, **241**, 2629-2642.

[8] Danay, A. (2012) "Response of steel-concrete composite panels to in-plane loading," *Nuclear Engineering and Design*, **242**, 52-62.

[9] Varma, A. H., S.R. Malushte, K.C. Sener, and Z. Lai (2014) "Steel-plate composite (SC) walls for safety related nuclear facilities: Design for in-plane forces and out-of-plane moments," *Nuclear Engineering and Design*, **269**, 240-249.

[10] Epackachi, S., A.S. Whittaker, A.H. Varma, and E.G. Kurt (2015a) "Finite element modeling of steel-plate concrete composite wall piers," *Engineering Structures*, **100**, 368-384.

[11] Epackachi, S., A.S. Whittaker, and Y-N. Huang (2015b) "Analytical modeling of rectangular SC wall panels," *Journal of Constructional Steel Research*, **105**, 49-59.

[12] Seo, J., A.H. Varma, K. Sener, and D. Ayhan (2016) "Steel-plate composite (SC) walls: In-plane shear behavior, database and design," *Journal of Constructional Steel Research*, **119**, 202-215.

[13] Kurt, E. G., A.H. Varma, P. Booth, and A.S. Whittaker (2016) "In-Plane Behavior and Design of Rectangular SC Wall Piers without Boundary Elements," *Journal of Structural Engineering* (ASCE), **142**(6), 04016026.

[14] Yan, J-B., and J.Y.R. Liew (2016) "Design and behavior of steel–concrete–steel sandwich plates subject to concentrated loads," *Composite Structures*, **150**, 139-152.

[15] Eom, T-S., H-G. Park, C-H. Lee, J-H. Kim, and I-H. Chang (2009) "Behavior of double skin composite wall subjected to in-plane cyclic loading," *Journal of Structural Engineering* (ASCE), **135**(10), 1239-1249.

[16] Hu, H-S., J-G. Nie, and M.R. Eatherton (2014) "Deformation capacity of concrete-filled steel plate composite shear walls," *Journal of Constructional Steel Research*, **103**, 148-158.

[17] Nie, J-G., H-S. Hu, J-S. Fan, M-X. Tao, S-Y. Li and F-J. Liu (2013) "Experimental study on seismic behavior of high-strength concrete filled double-steel-plate composite walls," *Journal of Constructional Steel Research*, **88**, 206-219.

[18] Nie, J-G., X-W. Ma, M-X. Tao, J-S. Fan, and F-M. Bu (2014) "Effective stiffness of composite shear wall with double plates and filled concrete," *Journal of Constructional Steel Research*, **99**, 140-148.

[19] Chen, L., Mahmoud, H., Tong, S-M., and Y. Zhou (2015) "Seismic behavior of double steel plate–HSC composite walls," *Engineering Structures*, **102**, 1-12.

[20] Ji, X., X. Cheng, X. Jia, and A. H. Varma (2017) "Cyclic In-plane Shear Behavior of Double-skin Composite walls in High-Rise Buildings," *Journal of Structural Engineering* (ASCE), **143**(6), 04017025.

[21] Zhao, W., Q. Guo, Z. Huang, L. Tan, J. Chen, and Y. Ye (2016) "Hysteretic model for steel–concrete composite shear walls subjected to in-plane cyclic loading, *Engineering Structures*, **106**, 461-470.

[22] Zhang, K., A.H. Varma, S.R. Malushte, and S. Gallocher (2014) "Effect of shear connectors on local buckling and composite action in steel concrete composite walls," *Nuclear Engineering and Design*, **269**, 231-239.

[23] Lanning, J., Benzoni, G. and Uang, C.M. (2016) "Using buckling-restrained braces on long-span bridges. II: Feasibility and development of a near-fault loading protocol," *Journal of Bridge Engineering*, 21(5), 04016002.

